RSC Advances

PAPER

View Article Online
View Journal | View Issue

Cite this: *RSC Adv.*, 2014, **4**, 13293

A new organic–inorganic hybrid electrolyte based on polyacrylonitrile, polyether diamine and alkoxysilanes for lithium ion batteries: synthesis, structural properties, and electrochemical characterization†

Yu-Chi Pan,[a] Diganta Saikia,[a] Jason Fang,[b] Li-Duan Tsai,[b] George T. K. Fey[c] and Hsien-Ming Kao*[a]

A new type of organic–inorganic hybrid polymer electrolyte based on poly(propylene glycol)-*block*-poly(ethylene glycol)-*block*-poly-(propylene glycol)bis(2-aminopropyl ether), polyacrylonitrile (PAN), 3-(glycidyloxypropyl)trimethoxysilane (GLYMO) and 3-(aminopropyl)trimethoxysilane (APTMS) complexed with $LiClO_4$ *via* the co-condensation of organosilicas was synthesized. The structural and electrochemical properties of the materials were systematically investigated by a variety of techniques including differential scanning calorimetry (DSC), Fourier transform infrared spectroscopy (FTIR), multinuclear (^{13}C, ^{29}Si, ^{7}Li) solid-state NMR, AC impedance, linear sweep voltammetry (LSV) and charge–discharge measurement. A maximum ionic conductivity value of 7.4×10^{-5} S cm^{-1} at 30 °C and 4.6×10^{-4} S cm^{-1} at 80 °C is achieved for the solid hybrid electrolyte. The ^{7}Li NMR measurements reveal the strong correlation of the lithium cation and the polymer matrix, and the presence of two lithium local environments. After swelling in an electrolyte solvent, the plasticized hybrid membrane exhibited a maximum ionic conductivity of 6.4×10^{-3} S cm^{-1} at 30 °C. The good value of the electrochemical stability window (~4.5 V) makes the plasticized hybrid electrolyte membrane promising for electrochemical device applications. The preliminary lithium ion battery testing shows an initial discharge capacity value of 123 mA h g^{-1} and a good cycling performance with the plasticized hybrid electrolyte.

Received 17th December 2013
Accepted 24th February 2014

DOI: 10.1039/c3ra47695b

www.rsc.org/advances

Introduction

In recent years, the worldwide energy crisis due to over-exploitation of fossil fuels and an increase in environmental pollution which is related to global warming have drawn the attention of the scientific community towards the development of efficient and reliable electrochemical devices. For an efficient system, improvement in the electrochemical device components is prerequisite. Ion conducting polymer electrolyte which is an indispensable component in electrochemical devices, such as lithium ion batteries, dye-sensitized solar cell, supercapacitors, electrochromic displays, *etc.*, is actively studied for many decades.[1–4] The field of polymer electrolytes has gone through various developmental stages, *e.g.*, from dry solid polymer electrolytes (SPEs) to gel, rubbery, and micro/nano-composite polymer electrolytes.[5] SPEs have been considered as safer alternatives to organic liquid electrolytes as the disadvantages like liquid leakage, volatility and flammability which associated with the liquid electrolytes are absent from SPEs.[6,7] Moreover, SPEs are flexible, cost effective and have high dimensional stability and safety that could lead to the elimination of separators used in batteries. SPEs based on polyethers dissolved metal salts have been widely investigated, and attention has been focused mostly on poly(ethylene oxide) (PEO) based systems.[8,9] However, the ionic conductivity of PEO based polymer electrolytes is comparatively lower except at high temperatures. To overcome this critical shortage, several strategies have been developed to suppress the PEO crystallization and to increase the amorphous phase, which allows the charge carriers to orientate through the polymer chains *via* liquid-like motion in the PEO based polymer electrolytes. Many attempts have been made to modify the polymer matrices by blending,

[a]*Department of Chemistry, National Central University, Chung-Li, Taiwan 32054, Republic of China. E-mail: hmkao@cc.ncu.edu.tw; Fax: +886-3-4227664; Tel: +886-3-4275054*

[b]*Department of Fuel Cell Materials and Advanced Capacitors, Division of Energy Storage Materials and Technology, Material and Chemical Laboratories, Industrial Technology Research Institute, Hsin-Chu 300, Republic of China*

[c]*Department of Chemical and Materials Engineering, National Central University, Chung-Li, Taiwan 32054, Republic of China*

† Electronic supplementary information (ESI) available: FTIR spectra of PAGE-*x* hybrid electrolytes, FTIR deconvolution results of PAGE-*x* hybrid electrolytes in the range of 600–650 cm^{-1} with various amounts of Li salt, depolarization curve of PAGE-24 hybrid electrolyte. See DOI: 10.1039/c3ra47695b

using block copolymers and crosslinking networks or dispersing nanosized ceramic fillers, such as SiO_2, TiO_2 or Al_2O_3, in the polymer matrix to inhibit chain crystallization and succeeded to enhance the ionic conductivity.[10–13] A more favorable strategy is to develop organic–inorganic hybrid electrolytes *via in situ* formation of inorganic component within the polymer matrix.[14–16] The combination of organic and inorganic components in the hybrid materials take advantages of the silicon based structure networks to provide a stable three dimensional framework, which offers enhanced mechanical properties to the hybrid materials. On the other hand, the polyacrylonitrile (PAN) based system has shown great potentials because of its high thermal stability and better mechanical strength than the PEO based system to be used as a separator in lithium polymer batteries.[17,18] Structurally, PAN has a continuous carbon backbone structure with the nitrile side groups. The nitrile side groups may help to enhance the solubility of lithium salt. To the best of our knowledge, there is no report on the reaction of PAN with the amine terminated triblock copolymer (NH_2–PPG–PEG–PPG–NH_2) using organosilanes as crosslinking agents.

In the present study, we synthesized a series of comb-like hybrid polymer electrolytes with cross-linked silica domains. The electrolytes were prepared *via* co-condensation of two organosilane precursors, which involved the reaction of polyacrylonitrile with (3-aminopropyl)trimethoxysilane (APTMS), denoted as precursor A, and the reaction of the polyether diamine with (3-glycidyloxypropyl)trimethoxysilane (GLYMO), denoted as precursor B. The physical and electrochemical properties of the hybrid electrolytes were investigated by differential scanning calorimetry (DSC), FTIR, solid-state NMR, alternating current (AC) impedance and linear sweep voltammetry measurements. Charge–discharge measurement was carried out to evaluate the performance of the electrolyte for possible Li-ion battery application.

Experimental section

Materials

PAN (Scientific polymer products Inc., $M_w = 150\,000$ g mol^{-1}), lithium perchlorate ($LiClO_4$, Aldrich), and triblock copolymer H_2N–$(PPG)_x(PEG)_{39}(PPG)_{6-x}$–$NH_2$, (Jeffamine ED2003, Aldrich, $M_w = 2000$ g mol^{-1}) were dried at 70 °C for 24 h under vacuum (<10^{-3} Torr) prior to their use. The bridging agents GLYMO (Aldrich) and APTMS (Aldrich) were used as received. *N*,*N*-Dimethylformamide (DMF, Aldrich) was used as the solvent.

Preparation of hybrid electrolytes

Scheme 1 illustrates the synthesis of organic–inorganic hybrid electrolytes in the present study. The preliminary step of the preparation of precursor A with a long chain amorphous polymer involves the reaction of the nitrile groups from PAN and the terminal amine groups of APTMS with a molar ratio of 5 : 1. In a typical synthesis, 0.25 g of PAN was mixed with 0.16 g of APTMS in a DMF solution (20 mL). The resulting solution was stirred at 55 °C for 12 h to yield a cross-linked hybrid precursor A, as illustrated in Scheme 1. On the other hand, the precursor B was prepared by mixing 0.42 g of GLYMO and 1.86 g of ED2003 in a DMF solution with a mole ratio of 2 : 1 and stirred at 55 °C for 12 h. Both the precursors were then mixed under constant stirring and 0.3 mL of 2 M HCl was added dropwise to catalyze the hydrolysis and condensation reactions of the organosilane for the formation of the silicate framework. The final solution was stirred at 55 °C for 24 h. Afterwards, an appropriate amount of $LiClO_4$ was added into the solution and stirred at 55 °C for 12 h. Finally, the resulting solution was cast onto Teflon dishes, and the solvent was slowly evaporated at room temperature for 48 h. The materials were then heated gradually from 30 °C to 75 °C under vacuum for several days to get transparent and crack-free films with good mechanical strength. The resulting hybrid electrolytes were designated as PAGE-*x*, where P stands for PAN, A for APTMS, G for GLYMO, E for Jeffamine ED2003 and *x* represents the weight of lithium perchlorate (in a factor of 10^{-2} g, *i.e.*, for $x = 15$, the weight of $LiClO_4$ is 0.15 g). The thickness of the films was controlled to be in the range of 80–100 μm. The cross-linked hybrid electrolyte films were strong and highly elastic in nature.

To prepare the plasticized organic–inorganic hybrid electrolyte, the salt free solid hybrid membrane (*i.e.*, without $LiClO_4$ salt), namely PAGE-0, was directly swelled in electrolyte solvents, such as 1 M $LiClO_4$ in EC–PC (1 : 1, v/v), 1 M LiTFSI in EC–PC (1 : 1, v/v) and 1 M $LiPF_6$ in EC–DEC (1 : 1, v/v). The thickness of the plasticized hybrid electrolyte membranes was controlled to be in the range of 50–70 μm.

Characterization methods

DSC studies were performed in the temperature range of −60 °C to 120 °C using a calorimeter (Perkin-Elmer Pyris 6 DSC) at a heating rate of 10 °C min^{-1}. The sample weights were maintained in the range of 3–5 mg, and all experiments were carried out under a nitrogen flow. The glass transition temperatures (T_g) and melting temperatures (T_m) were measured, and the associated enthalpy changes (ΔH) were calculated. Glass transition temperatures were reported as the midpoint of the transition process.

FTIR spectra were obtained from a spectrometer (Bio-Rad FTS155) at a resolution of 4 cm^{-1} using the KBr wafer technique. Band deconvolution of the resulting spectra in the range of 600–650 cm^{-1} was conducted to obtain the best fit for the band envelope.

AC impedance measurements of the hybrid electrolytes were performed using a frequency response analyzer (Autolab/PGSTAT302, Metrohm Autolab B.V., Netherlands) over a frequency range of 1 MHz to 1 Hz with an amplitude of 10 mV. All the samples were sandwiched by two polished stainless steel blocking electrodes in an argon atmosphere inside a glove box (Innovative technology, PL-HE-2GB with PL-HE-GP1 inert gas purifier) for conductivity tests. The measurements were performed in the temperature range of 20–85 °C. Each sample was thermally equilibrated at each selected temperature for at least 30 min prior to taking measurements. Complex impedance plots (semi-circles) were computed from the experimental data.

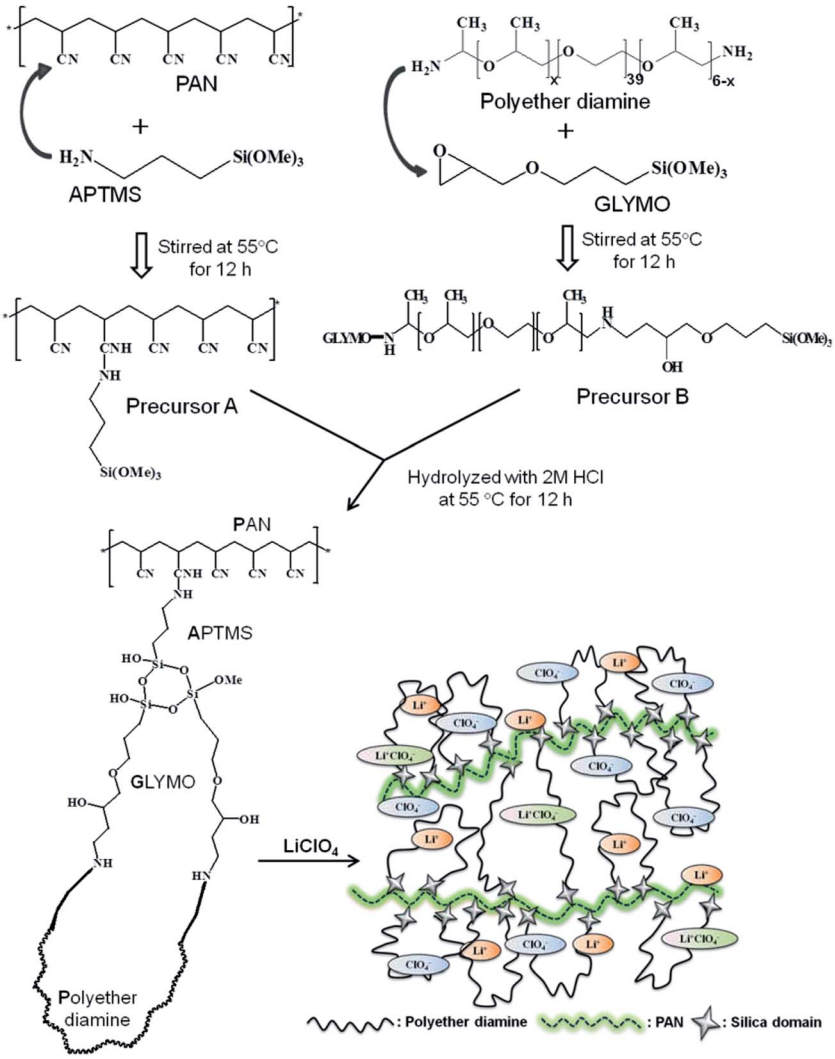

Scheme 1 Schematic diagram of the synthesis of the PAGE-*x* hybrid electrolytes.

The intercept at the real impedance axis in the Nyquist plots corresponds to the bulk electrolyte resistance (R_b) and hence the ionic conductivity values (σ) are obtained from equation $\sigma = (1/R_b)(t/A)$, where t is the thickness of the electrolyte film and A is the area of the electrode.

The Li transference numbers (t_+) of solid hybrid electrolytes were determined by using a combination method of dc polarization and AC impedance measurements, which has been reported by Evans *et al.*[19] The current and resistance were measured by an impedance analyzer (Autolab/PGSTAT302). The sample was assembled in a coin-cell holder using lithium foils as non-blocking electrodes in an argon gas-filled glove box. Finally, it was placed into an oven, which was held the temperature at 70 °C. The dc voltage pulse applied to the cell was 10 mV.

Linear sweep voltammetry (LSV) measurements were carried out in both solid hybrid electrolytes with various salt concentrations and plasticized hybrid electrolytes with different electrolyte solvents. A standard 2032 coin-cell hardware was used for cell fabrication. Both the PAGE-*x* and PAGE-0 hybrid membranes were dried overnight at 70 °C in an oven and placed into an argon-filled glove box that contained <1 ppm oxygen and moisture. The PAGE-0 membranes were soaked in the electrolyte solutions for 30 min. The electrochemical stability of the electrolyte was determined by LSV using stainless steel (SS) as working electrode and lithium foil as counter and reference electrodes for a Li/solid (or plasticized) hybrid electrolyte/SS cell at a scan rate of 1 mV s^{-1} from 0 to 6 V *vs.* Li/Li^+.

Charge–discharge studies were carried out with an automatic battery cycler (WonATech WBCS3000). Lithium metal (Alfa Aesar) and $Li(Ni_{0.4}Mn_{0.4}Co_{0.2})O_2$ (NMC-442, Industrial Technology Research Institute, Taiwan) were used as the anode and cathode, respectively. The cathode was prepared by blade-coating a slurry of 88 wt% NMC-442, 3 wt% Super P carbon, 3 wt% carbon black and 6 wt% poly(vinylidene fluoride) (PVdF) binder in *N*-methyl-2-pyrrolidone (NMP) on aluminum foil, drying overnight at 120 °C in an oven, roller-pressing the dried coated foil, and punching out circular discs. The cycle tests of normal charge were carried out at a 0.2 C-rate between 2.8 and 4.0 V.

Solid-state NMR experiments were performed on a NMR spectrometer (Varian Infinityplus-500), equipped with a Chemagnetics

7.5 mm magic angle spinning (MAS) probe. The Larmor frequencies for ^{7}Li, ^{13}C and ^{29}Si nuclei are 194.3, 125.7 and 99.3 MHz, respectively. The Hartmann–Hahn matching conditions for ^{1}H → ^{13}C and ^{1}H → ^{29}Si cross polarization (CP) MAS experiments were determined using admantane and octakis(trimethylsiloxy)silsesquioxane (Q_8M_8), respectively. The ^{13}C and ^{29}Si chemical shifts were externally referenced to tetramethylsilane (TMS) at 0 ppm. ^{7}Li NMR spectra were acquired under MAS condition during the acquisition. ^{7}Li chemical shifts were externally referenced to a 1 M aqueous solution of LiCl at 0 ppm.

Results and discussion

Thermal properties of solid hybrid electrolytes

Ionic migration is governed by chain flexibility in the polymer matrix, and the increase in chain flexibility may assist ion transport in polymer electrolytes. Normally, migration is affected by at least two factors: (i) the mobility of the polymer chains and (ii) the interaction of Li cations with anions and polymer chains.[20] Generally, the lower the T_g values, the higher the mobility of the polymer chains. Fig. 1 shows the DSC thermograms of pure ED2003, PAN and the PAGE-*x* hybrid electrolytes with various salt concentrations, and the results are summarized in Table 1. As seen in Fig. 1 and Table 1, the T_g values of the PAGE-27 and PAGE-30 electrolytes increase with the increase in lithium salt concentrations. The interaction between the oxygen atoms of the polyether units and the lithium cations results in the progressive increase of T_g of the complex, which in turn decreases the mobility of the polymer chains.[16] The T_g values for pure ED2003, PAGE-0, and PAGE-*x* (x = 15–24) were not possible to be measured because of the limitation of instrument (Perkin Elmer Intracooler, model no. FC100PEA2) in cooling below −60 °C.

The ED2003 has a melting transition at 35.4 °C, while PAN has no melting transition within the temperature range studied. After reacting with the organosilane and PAN, the T_m value of the PAGE-0 (without Li salt) sample shifted slightly to 34.1 °C and down further to 25.5 °C after doping with lithium salt. Besides, a small melting peak was observed around 5 °C when the doping amount of lithium salt was increased. The coordination of lithium cations with the –CN groups of PAN and –C–O–C– units of ED2003 may cause a different crystalline environment of polyesters. The area under the curve for the melting endotherm in DSC data is directly related to the crystallinity of the electrolyte sample. The percentage of crystallinity (χ_c) of the hybrid electrolytes was estimated by using the equation,

$$\chi_c = \frac{\Delta H}{\Delta H_f} \times 100\% \quad (1)$$

where ΔH_f is the enthalpy of fusion of pure ED2003 and ΔH is the enthalpy of fusion of hybrid polymer electrolyte. The PAN polymer exhibits complete amorphous nature. Table 1 lists the changes in the degree of the crystallinity of the hybrid polymer electrolytes. It was found that the degree of crystallinity of the polymer electrolytes decreased with the increase in the salt concentrations, suggesting that the increased interaction of the lithium cations with the oxygen atoms of PEG–PPG destroyed the regular crystallized polymer framework and increased the amorphous phase in the polymer complex. An exothermic peak in the temperature range of −4 to +7 °C, corresponding to the recrystallization of the parent polymer ED2003 was observed for the PAGE-27 and PAGE-30 samples.[21]

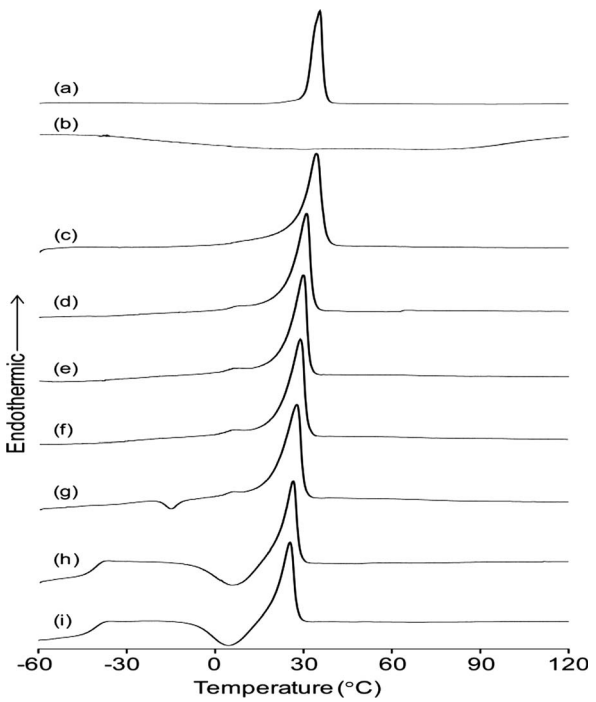

Fig. 1 DSC thermograms of pure ED2003 (a), PAN (b) and PAGE-*x* hybrid electrolytes with various amounts of Li salt, where x = 0 (c), 15 (d), 18 (e), 21 (f), 24 (g), 27 (h), and 30 (i).

Li^+–polymer interactions

Infrared spectroscopy is employed to provide the information about the structure of organic–inorganic hybrid and the interaction of the polyether and cyano groups with the lithium salt. FTIR spectra of the PAGE-*x* hybrid electrolytes with various amounts of lithium salt are shown in Fig. S1 (ESI†). According to the literature, the broad band in the region of 3500–3300 cm^{-1} was due to the N–H stretching vibration.[22] The bands at 2915 and 2875 cm^{-1} were due to the asymmetric and symmetric CH_2 stretching vibrations of ED2003 and PAN, respectively. The bands at 1250 and 1040 cm^{-1} are assigned to the C–N in-plane symmetric and C–C symmetric stretching vibrations of PAN, respectively.[23] The vibrational band in the region of 2280–2220 cm^{-1} was deconvoluted and found two contributions, the free C≡N at 2242 cm^{-1} and the bonded C≡N at 2262 cm^{-1}, as shown in Fig. 2. The coordination between the C≡N group of PAN and the lithium cations is responsible for the shoulder at 2262 cm^{-1}.[24] The percentage of the bonded C≡N groups is slightly increased from 4.6% to 7.7% with the increase in the amount of lithium salt. As the structure of PAN involves only the C–C backbone and the C≡N side groups, the changes in the intensity of C≡N vibration bands with the increase in the salt

Table 1 Glass-transition temperature (T_g), melting temperature (T_m), endothermic heat (ΔH), crystallinity (χ_c), ionic conductivity (σ), activation energy (E_a) and transference number (t_+) of PAGE-x solid hybrid electrolytes

Sample	T_g (°C)	T_m (°C)	ΔH (J g^{-1})	χ_c[a] (%)	σ (S cm^{-1}, 30 °C)	E_a (eV)	t_+
ED2003	—	35.4	102.0	100	—	—	—
PAN	110.2	—	—	—	—	—	—
PAGE-0	—	34.1	46.3	45.4	—	—	—
PAGE-15	—	30.8	39.1	38.3	4.6×10^{-5}	0.38	0.22
PAGE-18	—	29.8	37.9	37.2	5.2×10^{-5}	0.39	0.24
PAGE-21	—	28.8	36.6	35.9	5.6×10^{-5}	0.35	0.26
PAGE-24	—	27.5	30.9	30.2	7.4×10^{-5}	0.35	0.3
PAGE-27	−41	26.3	23.3	22.8	3.2×10^{-5}	0.42	0.25
PAGE-30	−39	25.5	13.5	13.2	—	—	—

[a] Assuming the crystallinity of ED2003 is 100%.

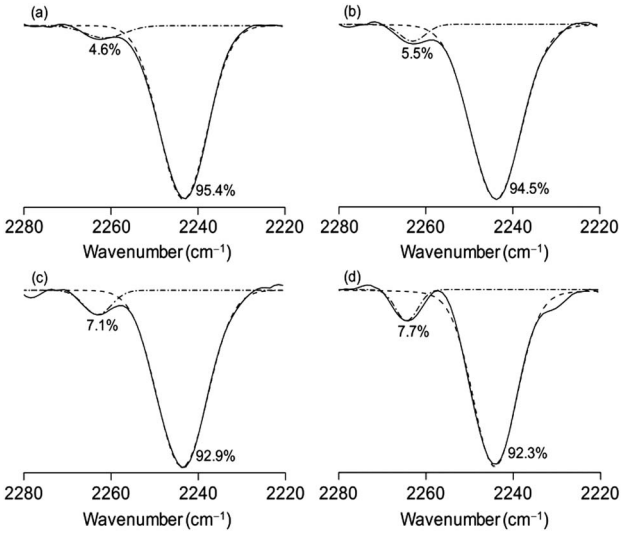

Fig. 2 FTIR deconvolution results of PAGE-x hybrid electrolytes in the range of 2220–2280 cm^{-1} with various amounts of Li salt, where x = 15 (a), 18 (b), 21 (c), and 24 (d).

concentration suggest the increased interaction of Li^+ ions with the C≡N groups.[25] The band at 1653 cm^{-1} was considered to be the C=N stretching vibration band of the CN groups reacted with the amine group of APTMS.[26] The N–H bending and C–N stretching vibration bands were observed at 1558 cm^{-1} and 1510 cm^{-1}, respectively. The peaks at 1455, 1350, 1300, 1250 and 850 cm^{-1} were assigned to –CH_2 bending, wagging, twisting and rocking vibrations of ED2003, respectively.[27,28] A major peak associated with the C–O–C stretching vibrations was observed at 1106 cm^{-1} for ED2003. With the addition of the lithium salt, two peaks at 1120 and 1107 cm^{-1} appeared, indicating that the ether groups of ED2003 had some interactions with the added lithium salt. Although the changes in the intensity, shape, and position of the C–O–C stretching mode were associated with the polyether–$LiClO_4$ interactions, the dependence of the vibrational peaks of C–O–C on the salt concentrations was not clarified in FTIR spectra, since the characteristic vibration bands of the hydrolysis product (Si–O–Si and Si–O–C) of GLYMO were also expected to appear in the same region. The typical vibration band for noncondensed Si–OH was found at 950 cm^{-1}.

The fraction of free ions which can transport effectively is an important parameter for ionic conduction. In particular, the $\nu(ClO_4^-)$ mode provides the information about the estimation of free ions. Deconvoluting the peak around 600 to 650 cm^{-1} for the PAGE-x hybrid electrolytes, two bands at 625 and 635 cm^{-1} were observed. The band centered at 625 cm^{-1} has been assigned to the vibration of the free ClO_4^- anions, which does not directly interact with the lithium cations, and the band centered at 635 cm^{-1} to the vibration of $Li^+ClO_4^-$ contact ion pairs.[29] To investigate the behavior of ion association in the present electrolyte system, the spectral features of $\nu(ClO_4^-)$ mode were fitted with Gaussian–Lorentzian functions. As shown in Fig. S2 (ESI),† the fraction of free anions decreases with increasing salt concentrations, *i.e.*, the number of free lithium ions decreases with increasing salt concentrations as well. About 84% of ClO_4^- exists as spectroscopically free species for PAGE-15, while only 75–79% of free ClO_4^- is observed for the other PAGE-x (x = 18, 21, 24) electrolyte samples. Although these numbers are not remarkably different, there is a clear difference in values between PAGE-15 and other electrolytes, as shown in Fig. S2.† Given that the triblock polymer has poor ability to dissolve salt, the present electrolyte system consisting of polyacrylonitrile incorporated with ED2003 has a high degree of ionic dissolution, suggesting that the extent of the interaction of the lithium cations and the C≡N groups provide more hopping and coordinating sites to the lithium cations, resulting in an enhancement of the ionic movement.

Structure of polymer backbone

Solid-state ^{13}C CPMAS NMR studies were performed to determine the structure of the organic part of the polymer electrolyte system. Fig. 3A shows the ^{13}C CPMAS NMR spectra of the PAGE-x hybrid electrolytes acquired at a contact time of 3 ms. The dominant peak at 70 ppm is assigned to the methylene carbons adjacent to the ether oxygens of the ED2003 polymer chains, while the peak at 17 ppm is due to the CH_3 groups of PPG chains. Besides the major peak at 70 ppm, there is a smaller peak at 75 ppm due to the ether carbons in the PPG segments. The other dominant peak at 30 ppm is assigned to the C–H backbone of PAN. The C≡N side groups exhibit a peak at 120 ppm. As the C≡N group reacts with the NH_2 group of APTMS,

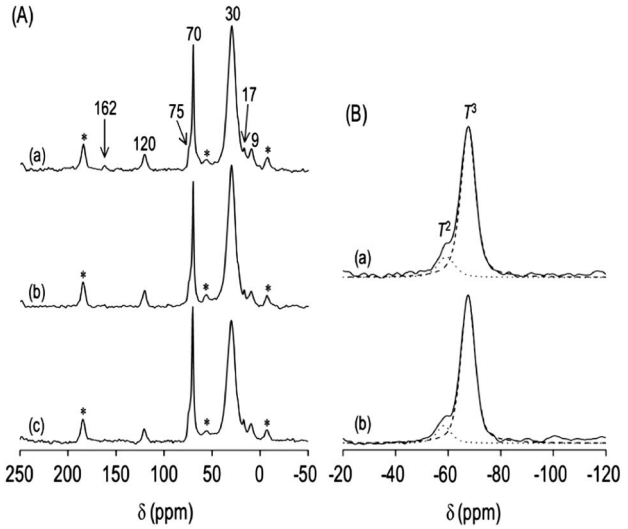

Fig. 3 (A) ^{13}C CPMAS NMR spectra of PAGE-x hybrid electrolytes, where $x = 18$ (a), 21 (b), and 24 (c), acquired at a spinning speed of 8 kHz. Asterisks denote spinning sidebands. (B) ^{29}Si CPMAS NMR spectra of PAGE-x hybrid electrolytes with $x = 18$ (a) and 24 (b).

the peak observed at 162 ppm indicates that the C═N–R groups are successfully formed for the PAGE-x electrolytes. The shoulder peak at 44 ppm that overlaps with the peak at 30 ppm can be assigned to the carbon atom next to the nitrogen atom in APTMS or the nitrogen substituted carbons at the terminal of the ED2003 diamine. Two peaks at 22 and 9 ppm are assigned to the methylene carbons in the α and β positions to the silicon atom of GLYMO, respectively. The linewidth of the peak at 30 ppm (from PAN) is significantly larger as compared to the peak at 70 ppm (from ED2003), suggesting that the chain mobility of ED2003 is higher than PAN.

Silicate framework of the hybrid electrolytes

^{29}Si CPMAS NMR measurements were carried out to investigate the silicate network architecture inside the organic–inorganic electrolyte systems. As shown in Fig. 3B, two peaks at −67 and −59 ppm corresponding to T^3 ($RSi(OSi)_3$, R = alkyl group) and T^2 ($RSi(OSi)_2(OH)$) sites, respectively, were observed for the two selected PAGE-18 and PAGE-24 samples. The observation of T groups indicates the presence of organosilane groups in the electrolyte system. The spectral features for both samples are essentially the same, indicating the condensation of silicate network is not significantly affected by the different amount of Li salt. The $T^2 : T^3$ ratios were 14 : 86 for PAGE-18 and 12 : 88 for PAGE-24. As the percentage of T^3 was higher than T^2, the organosilane groups were well condensed and the amount of silanol groups (Si–OH) was much lower. The significant populations of T^3 groups indicate a high degree of crosslinked structure with enhanced mechanical strength.

Ionic conductivity of solid hybrid electrolytes

It is generally accepted that ionic conductivity in polymer electrolytes is mainly attributed to a property of amorphous phase above their glass transition temperatures. Fig. 4 shows the temperature dependence of the ionic conductivity of PAGE-x hybrid electrolytes. The variation of conductivity with temperatures suggests a Vogel–Tammann–Fulcher (VTF) like behavior, indicating that the ion transport in the present hybrid electrolytes is mainly dependent on the polymer segmental motion. Although the conductivity plot suggested curve profile and necessitated to interpret the data with VTF equation, it was not possible to fit in the VTF equation, as the T_g of the most of the hybrid electrolytes was not possible to measure because of the limitation of DSC instrument measuring below −60 °C. Generally, the ionic conductivity (σ) of a polymer electrolyte depends on the actual concentration of the conducting species and their migration as

$$\sigma(T) = \sum_i n_i q_i \mu_i \quad (2)$$

where n_i is the number of charge carriers, q_i is the charge on each charge carrier, and μ_i is the mobility of charge carriers. i is the ionic species which are mainly cations and anions that contribute to the total conductivity. Normally, the conductivity increases with the increase in salt concentrations as the total number of charge carriers increases. However, as the salt concentration increases, the formation of associated ionic species (*e.g.*, contact ion pairs, solvent separated ion pairs or higher ion aggregates) also increases, which reduces the overall migration and the number of effective charge carriers, and hence the decrease in ionic conductivity is often observed at high salt concentrations. As seen in Fig. 4, the ionic conductivity increases with increase in the salt concentration from PAGE-15 to PAGE-24 and then slowly decreases for PAGE-27. The PAGE-24 sample exhibits the highest ionic conductivity values of 7.4×10^{-5} S cm^{-1} and 4.6×10^{-4} S cm^{-1} at 30 °C and 80 °C, respectively. Further increase or decrease in salt concentration results in the decrease in ionic conductivity. The activation energy (E_a) is calculated from the conductivity plot and the values are given in Table 1. As seen in Table 1, the activation energy increases with the increase in salt concentration, except

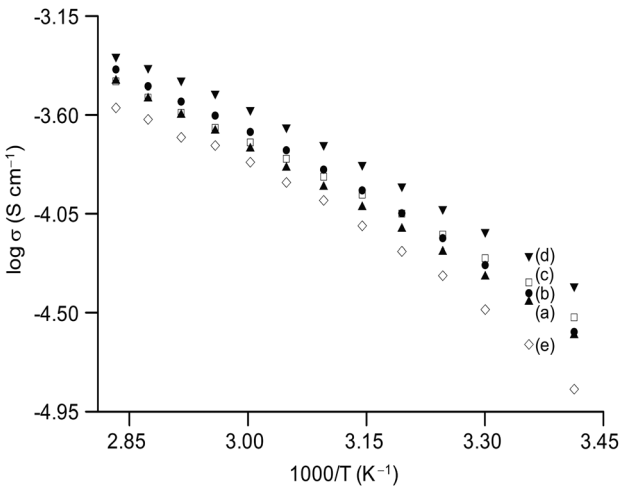

Fig. 4 Temperature dependence of ionic conductivity of PAGE-x hybrid electrolytes, where $x = 15$ (a), 18 (b), 21 (c), 24 (d), and 27 (e).

for the PAGE-21 and PAGE-24 samples. The comparatively lower E_a values for all the hybrid samples suggest the rapid diffusion of ionic charge carriers.[30,31] It is noticed that the lowest E_a value for PAGE-24 coincides with the highest ionic conductivity of this hybrid electrolyte. Moreover, the ionic conductivity increases with the increase in temperature, which can be explained by the free volume theory proposed by Cohen and Turnbull.[32,33] As the temperature is increased, the polymer can expand easily and produces free volumes. Therefore, the ions, solvated molecules, or the polymer segments can move into the free volume and travel freely and faster which helps in the enhancement of ionic conductivity.[34] The ionic conductivity increases with temperature for all the selected samples. Although PAGE-21 shows a higher ionic conductivity value than PAGE-18 at lower temperatures, its higher temperature conductivity is lower than PAGE-18. The slow rise in the conductivity for PAGE-21 at higher temperatures might be due to its slower growth of free volume. It suggested that the free volume may be surrounded by the hard segment of polymer, which prohibits the enlargement of free volume at a faster rate. As a result, this effect reduces the faster increase of ionic conductivity at higher temperatures for PAGE-21 than PAGE-18.

It has been reported that ionic conductivity may depend on the influence of the fillers on the mobility of both the polymer and the salt.[12,35,36] As the present organic–inorganic hybrid electrolyte produces *in situ* silica domains in the matrix, it can be considered as a two phase system consisting of an ionically conducting polymer matrix with dispersed silica networks. The ionic conductivity could arise from the existence of a highly conducting layer at the polymer–SiO_2 interface.[37] This interface layer could be an amorphous polymer layer surrounding SiO_2 and/or a space-charge layer.[38] The interface layers are the sites of high defect concentrations that may allow faster ion transport by serving as channels for conducting ions. Therefore, in the present PAGE-*x* hybrid system, these interface layers may also help by conducting ions to achieve the ionic conductivity values reported.

Transference number measurement of solid hybrid electrolyte

Li^+ transference number was measured in order to realize the cationic contribution in ionic conductivity. The lithium transference number (t_+) was determined by Evans *et al.* method as,[19]

$$t_+ = \frac{I_s(\Delta V - I_0 R_0)}{I_0(\Delta V - I_s R_s)} \quad (3)$$

where ΔV is the potential applied across the cell. I_0 and I_s are the initial and steady-state dc currents, and R_0 and R_s are the initial and steady-state resistances of the passivating layers. The result of Li^+ transference number for the PAGE-*x* solid hybrid electrolytes is given in Table 1 and the typical depolarization curve of the PAGE-24 sample is shown in Fig. S3 (ESI).† As evident from Fig. S3,† a progressive extension of the low frequency semi-circle can be easily observed, indicating an increase in the interfacial resistance, which in turn must be associated with the growth of a passivation layer on the lithium electrode.[39,40] The passive layer of the lithium electrode may contain the product of the corrosion reaction between the lithium electrode and the polymer, the salt, and other impurities. The steady state current observed in Fig. S3† is thus considered to result from the establishment of a concentration polarization of the anion and the growth of passivating layers. The Li^+ ions can interact not only with the ether oxygen atoms in PEG and PPG, but also with the oxygen atoms in ClO_4^-, therefore their transport abilities are restricted, which in turn result in a low t_+ value (<0.4) in the solid hybrid electrolytes.[13] As the measured transference number value is lower than 0.5, the anionic species are the main contributors to the total ionic conductivity.

Local environments of Li cations

There are three possible coordination sites for Li^+ cation in the present hybrid electrolyte structure: (i) the ether oxygen atoms of triblock polyether, (ii) the oxygen atoms of silica domains, and (iii) the nitrogen atoms of polyacrylonitrile. To identify and explore the local environments of the Li^+ cations in the present hybrid electrolytes, variable temperature ^7Li-{^1H} (*i.e.*, proton decoupled) MAS NMR measurements were performed on the PAGE-24 sample at a spinning speed of 3 kHz. As shown in Fig. 5, two ^7Li resonances at −1.0 ppm (site I) and −1.7 ppm (site II) were observed at −90 °C for PAGE-24.[41] The most intense peak at −1.0 ppm (site I) is assigned to the lithium cation coordinated with the oxygen atoms on the ether groups, whereas the peak at −1.7 ppm (site II) may be due to the lithium cation coordinated with the nitrogen atoms of polyacrylonitrile. The ether oxygen atoms in the PEG–PPG chain interact with the lithium cations more strongly than the nitrogen atom in polyacrylonitrile because of the higher donor number of the oxygen atom on PEG–PPG and thus exhibit a larger peak at site I.

Transformation of solid hybrid electrolytes to plasticized hybrid electrolytes

Although the present solid hybrid electrolytes are suitable for some electrochemical applications, it is not possible to use in

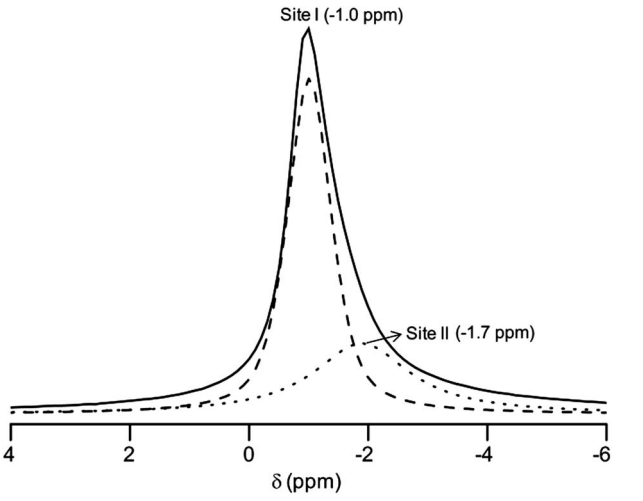

Fig. 5 ^7Li-{^1H} MAS NMR spectra of PAGE-24 hybrid electrolyte acquired at −90 °C and a spinning speed of 3 kHz.

lithium ion batteries due to their lower ionic conductivity values. To explore the possibility of the present hybrid electrolyte system to be applied in lithium ion batteries, attempt was therefore made to plasticize the solid salt free hybrid polymer membrane, that is, PAGE-0, with different organic electrolyte solvents to enhance the ionic conductivity. The electrolyte solvents used in plasticized hybrid are 1 M $LiClO_4$–LiTFSI in EC–PC or 1 M $LiPF_6$ in EC–DEC. The results of DSC, FTIR, ^{13}C and ^{29}Si CPMAS NMR can also be applied to the plasticized hybrid electrolyte as they provide the structural information of the hybrid. Some necessary characterizations were carried out for the plasticized hybrid electrolytes with the purposes to evaluate their potentials in lithium ion battery application.

Swelling behavior and ionic conductivity of plasticized hybrid electrolytes

The salt free PAGE-0 hybrid sample was used for swelling ratio (SR) measurements. The swelling ratio of the PAGE-0 hybrid membrane was measured in different electrolyte solvents using the relation,

$$\mathrm{SR}\,(\%) = \frac{W - W_0}{W_0} \times 100 \qquad (4)$$

where W and W_0 are the weights of the wet and dry hybrid polymer membrane, respectively. Fig. 6A depicts the swelling behavior of PAGE-0 in different electrolyte solvents. As seen in Fig. 6A, the swelling ratios follow the order: 1 M $LiClO_4$ in EC–PC (1 : 1, v/v) > 1 M LiTFSI in EC–PC (1 : 1, v/v) > 1 M $LiPF_6$ in EC–DEC (1 : 1, v/v). The maximum swelling ratio of 120% is obtained for the PAGE-0 sample in 1 M $LiClO_4$ in EC–PC, but reduces to 115% for 1 M LiTFSI in EC–PC and 106% for 1 M $LiPF_6$ in EC–DEC. Within a short interval time of 5 to 10 min, all the hybrid electrolytes reached almost the highest saturated swelling values. The faster electrolyte uptake of the hybrid membrane may be due to the typical branched structure of the hybrid membrane, which helps to absorb electrolyte solvents quickly and efficiently.

The temperature dependence of ionic conductivity of the PAGE-0 hybrid electrolytes swelled in different electrolyte solvents are displayed in Fig. 6B. The plasticized hybrid electrolyte shows an Arrhenius-like enhancement of conductivity when the temperature is increased, indicating that ion transport is decoupled from the polymer segmental motion and thermally activated ionic hopping plays major role in ion transport. The maximum ionic conductivity of 6.4×10^{-3} S cm^{-1} was achieved for the plasticized hybrid electrolyte with 1 M $LiClO_4$ in EC–PC at 30 °C. The conductivity values of the plasticized hybrid electrolyte slowly decrease with 1 M LiTFSI in EC–PC (5.5×10^{-3} S cm^{-1}), and 1 M $LiPF_6$ in EC–DEC (5.3×10^{-3} S cm^{-1}). The high ionic conductivity for the PAGE-0 sample with 1 M $LiClO_4$ in EC–PC is mainly attributed to the high electrolyte uptake in comparison to other samples as observed from the values of swelling ratio. In addition, the dielectric constants and viscosity of the solvents play a distinctive role in achieving such conductivity values. The estimation of viscosities of the solvent mixture in 1 M solution of

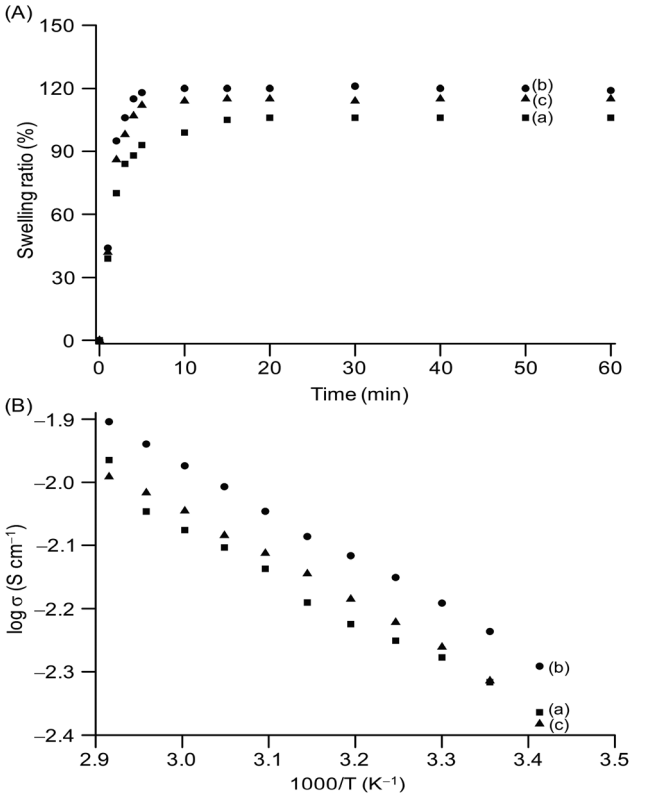

Fig. 6 Swelling behavior (A) and ionic conductivity (B) of PAGE-0 plasticized polymer electrolytes with 1 M $LiPF_6$ in EC–DEC (a), 1 M $LiClO_4$ in EC–PC (b) and 1 M LiTFSI in EC–PC (c).

salts is carried out to get an idea on the variation of ionic conductivity with different electrolyte solvents. Although the EC–DEC mixture has low viscosity (η(EC) = 1.9 cP and η(DEC) = 0.75 cP, η of the mixture = 1.325 cP) in comparison to EC–PC (η(EC) = 1.9 cP and η(PC) = 2.53 cP, η of the mixture = 2.215 cP),[6] DEC may not be totally compatible with the hybrid polymer structure. Further, the molecular size of DEC is larger than EC and PC, which may influence the absorption of electrolyte solvents by the PAGE-0 membrane. Hence, a lower electrolyte uptake is obtained with EC–DEC than with EC–PC, which results in a lower ionic conductivity with EC–DEC than EC–PC. Moreover, the dielectric constant of the solvent plays a role in the conductivity values. The lower ionic conductivity of the membrane with the $LiPF_6$ salt is attributed to the low dielectric constant of DEC ($\varepsilon = 2.82$) in comparison to PC ($\varepsilon = 64.4$). The dielectric constant of the binary solvent mixture of EC ($\varepsilon = 89$)–PC is about 76.7 and EC–DEC is 45.9.[42,43] The solvents with high dielectric constants dissociate the lithium salts more easily into free Li^+ ions, and thus help in the enhancement of ionic conductivity. On the other hand, as the dissociation constants of LiTFSI is higher than $LiClO_4$, the LiTFSI salt dissociates more easily than $LiClO_4$, resulting in enhancement of the viscosity of the 1 M LiTFSI in EC–PC in comparison to 1 M $LiClO_4$ in EC–PC.[44] Therefore, the ionic conductivity of the PAGE-0 sample with 1 M LiTFSI in EC–PC is lower than 1 M $LiClO_4$ in EC–PC. The liquid electrolyte is believed to be entrapped in the pores of the polymer matrix and then penetrated into the polymer

chains for swelling the amorphous domains.[45,46] Lithium ions can move through the polymer electrolyte in three ways, through liquid electrolyte stored in the pores, amorphous domains swelled by liquid electrolyte and along the polymer chains. The movement of lithium ions along polymer chains (dominant in the PAGE-*x* solid hybrid electrolyte) is much slower than movement through pores and amorphous domains as they get more free space to travel faster. The Arrhenius behavior of conductivity for this plasticized hybrid electrolyte also ruled out the possibility of segmental movement of polymer chains as the main cause of ion transport. Therefore, the pores filled with liquid electrolyte and swelled amorphous domains are the main transfer channels of lithium ions in the plasticized hybrid electrolytes. The PAGE-0 plasticized hybrid electrolyte membranes with different electrolyte solvents reached an ionic conductivity value as high as 10^{-2} S cm^{-1} at 70 °C, which is beneficial for applications in high temperature batteries.

Electrochemical stability of solid and plasticized hybrid electrolytes

The electrochemical stability of hybrid electrolyte is an essential parameter for providing a satisfactory performance in lithium ion batteries. Fig. 7A shows the linear sweep voltammograms of Li/PAGE-*x*/SS cells at a scan rate of 1 mV s^{-1} from 0 to 6 V *vs.* Li/Li$^+$. A low background current was measured in the potential region between 2.0 and 4.0 V for the PAGE-*x* hybrid electrolytes. This small current might be attributed to the change of the stainless steel surface.[47] A considerable current began to flow when the voltage crossed 4.0 V, indicating the onset of the decomposition process of the electrolyte. Therefore, the PAGE-*x* solid hybrid electrolytes are electrochemically stable up to 4.0 V.

The electrochemical stability window was also measured for the plasticized PAGE-0 hybrid electrolytes with different electrolyte solvents and depicted in Fig. 7B. As seen in Fig. 7B, the plasticized electrolyte membranes with 1 M $LiClO_4$ in EC–PC, 1 M LiTFSI in EC–PC and 1 M $LiPF_6$ in EC–DEC exhibit electrochemical stability windows of about 4.5 V. From these results, it is established that although solid hybrid electrolyte is acceptable with common intercalation compound cathodes like $LiCoO_2$, $LiFePO_4$, $LiMn_2O_4$, (working voltages in the range of 3.2–3.7 V) *etc.*, the plasticized hybrid electrolytes are more favorable for the practical application in lithium ion batteries.

Charge–discharge behavior of plasticized hybrid electrolyte

Although the ionic conductivity of the plasticized hybrid electrolyte membranes with the $LiClO_4$ and LiTFSI based salts were higher than the $LiPF_6$ based salt, for safety reason (*e.g.*, explosion of cell due to the strong oxidizing character of the salts) the standard procured electrolyte of 1 M $LiPF_6$ in EC–DEC was used for charge–discharge testing of the cell. Moreover, there is not much variation in conductivity values at 30 °C with these electrolytes. To evaluate the electrochemical performance of the lithium ion batteries with the hybrid electrolyte, Li/[PAGE-0 (1 M $LiPF_6$ in EC–DEC)]/NMC442 battery was assembled. The assembled battery was subjected to the cycle tests with an upper

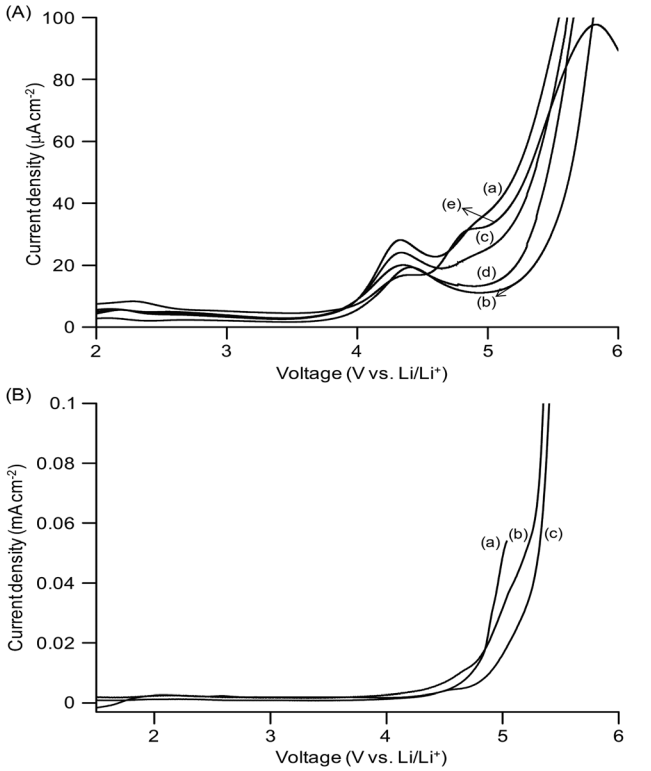

Fig. 7 Linear sweep voltammetry curves of the cells prepared with (A) PAGE-*x* hybrid electrolytes with *x* = 15 (a), 18 (b), 21 (c), 24 (d) and 27 (e), and (B) PAGE-0 plasticized hybrid electrolytes with 1 M $LiPF_6$ in EC–DEC (a), 1 M $LiClO_4$ in EC–PC (b) and 1 M LiTFSI in EC–PC (c).

voltage limit of 4.0 V and a lower voltage limit of 2.8 V at a current rate of 0.2 C. Fig. 8A shows the 1st, 5th and 15th cycle charge–discharge behavior of the lithium ion polymer battery. The coulombic efficiency of the first cycle was about 95%, which increased to 96.4% at 5th cycles and then slightly decreased to 92.5% at 15th cycles. The irreversible capacity loss observed in these cycles is caused by the formation of passivation film on the surface of the lithium electrode due to the decomposition of electrolyte. The formation of passivation layer consumes a part of the anode capacity corresponding to an irreversible capacity loss. The passive layer reduces the charge transfer in the lithium electrode and the diffusion rate of Li$^+$ ion in the Li/hybrid electrolyte interface becomes very slow.

The discharge capacity as a function of cycle number of the lithium ion battery with the PAGE-0 (1 M $LiPF_6$ in EC–DEC) hybrid electrolyte is shown in Fig. 8B. The initial discharge capacity of the cell is 123 mA h g^{-1} and then slowly decreases to 98 mA h g^{-1} at 20th cycle due to the formation of Li/hybrid electrolyte interface layer.[48] It suggests that the physical changes in the active materials and the passivation film on the surface of the electrode gradually increase the cell internal resistance during the cycling and block the charge transfer reaction between the Li electrode and the hybrid electrolyte, which results in the discharge capacity loss with cycling. The observed minor fluctuation in discharge capacity values with cycle numbers may be due to the unstable and non-uniform solid electrolyte interphase (SEI) layer. Although the upper cutoff

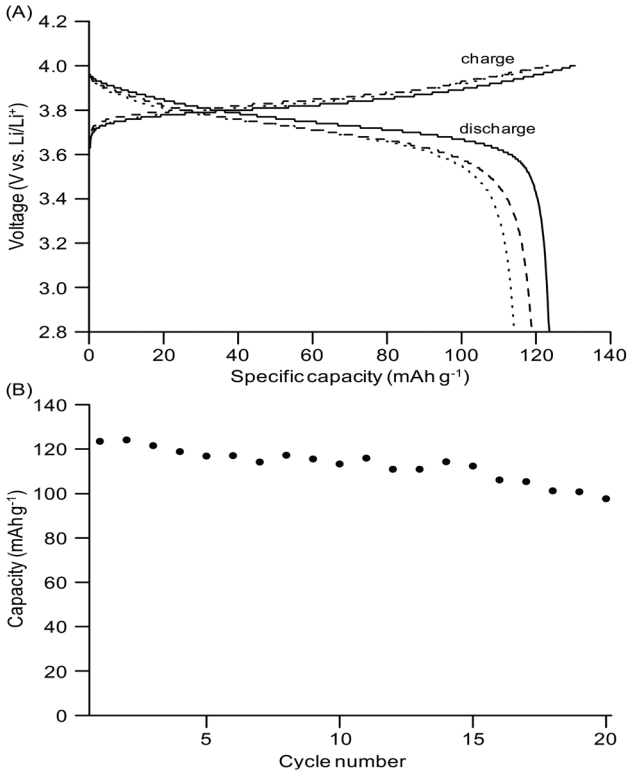

Fig. 8 (A) Galvanostatic charge–discharge curves of 1st (solid line), 5th (dashed line) and 15th (dot line) cycles for the Li/[PAGE-0 (1 M $LiPF_6$ in EC–DEC)]/NMC442 cell, and (B) discharge capacities of the cell as a function of cycle number.

voltage for Li/NMC442 cell can be set around 4.2 V, which would give a high capacity value, an upper cutoff voltage of 4.0 V is used in the present case as the higher cutoff voltage near the stability window may make the electrolyte unstable and deteriorate the charge–discharge performance. Since the main emphasis of the present study is to demonstrate the ability of the present hybrid electrolyte to be used in Li-ion battery systems, it is better to employ a lower voltage to restrain the plasticized hybrid electrolyte from any decomposition.

Conclusions

A new type of polyether diamine and polyacrylonitrile based hybrid polymer electrolytes was successfully synthesized. The addition of polyacrylonitrile in the polymer electrolyte system contributed to high dimensional stability and salt solubility. The maximum ionic conductivity of 7.4×10^{-5} S cm^{-1} was obtained for the solid hybrid electrolyte at 30 °C. Two local environments were identified in the present electrolyte by ^{7}Li-$\{^{1}H\}$ MAS NMR. The solid hybrid electrolyte exhibited a good electrochemical stability window of about 4.0 V *vs.* Li/Li^{+}. The plasticized hybrid electrolyte exhibited a high ionic conductivity value of 6.4×10^{-3} S cm^{-1} at 30 °C and good electrochemical stability window of about 4.5 V *vs.* Li/Li^{+}. The test cell carries an initial discharge capacity value of 123 mA h g^{-1} at 0.2 C. The characteristic electrochemical properties unfold new possibilities for such types of organic–inorganic hybrid electrolytes for application in electrochromic devices and lithium-ion batteries.

Notes and references

1 D. G. Kim, J. Shim, J. H. Lee, S. J. Kwon, J. H. Baik and J. C. Lee, *Polymer*, 2013, **54**, 5812.
2 W. Kwon, Y. J. Chang, Y. C. Park, H. M. Jang and S. W. Rhee, *J. Mater. Chem.*, 2012, **22**, 6027.
3 M. F. Hsueh, C. W. Huang, C. A. Wu, P. L. Kuo and H. Teng, *J. Phys. Chem. C*, 2013, **117**, 16751.
4 C. A. Nguyen, S. Xiong, J. Ma, X. Lu and P. S. Lee, *Phys. Chem. Chem. Phys.*, 2011, **13**, 13319.
5 J. R. MacCallum and C. A. Vincent, in *Polymer Electrolyte Reviews 1 and 2*, Elsevier, London, 1987 and 1989.
6 K. Xu, *Chem. Rev.*, 2004, **104**, 4303.
7 B. Dunn, H. Kamath and J.-M. Tarascon, *Science*, 2011, **334**, 928.
8 C. Berthier, W. Gorecki and M. Minier, *Solid State Ionics*, 1983, **11**, 91.
9 M. Armand, *Solid State Ionics*, 1994, **69**, 309.
10 Q. Xiao, X. Wang, W. Li, Z. Li, T. Zhang and H. Zhang, *J. Membr. Sci.*, 2009, **334**, 117.
11 T. Itoh, S. Gotoh, T. Uno and M. Kubo, *J. Power Sources*, 2007, **174**, 1167.
12 C. Tang, K. Hackenberg, Q. Fu, P. M. Ajayan and H. Ardebili, *Nano Lett.*, 2012, **12**, 1152.
13 F. Croce, G. B. Appetechi, L. Persi and B. Scrosati, *Nature*, 1998, **394**, 456.
14 L. M. Bronstein, R. L. Karlinsey, K. Ritter, C. G. Joo, B. Stein and J. W. Zwanziger, *J. Mater. Chem.*, 2004, **14**, 1812.
15 S. C. Nunes, V. de Zea Bermudez, M. M. Silva, S. Barros, M. J. Smith, E. Morales, L. D. Carlos and J. Rocha, *Solid State Ionics*, 2005, **176**, 1591.
16 D. Saikia, Y.-H. Chen, Y.-C. Pan, J. Fang, L.-D. Tsai, G. T. K. Fey and H.-M. Kao, *J. Mater. Chem.*, 2011, **21**, 10542.
17 T.-C. Wen, H.-H. Kuo and A. Gopalan, *Macromolecules*, 2001, **34**, 2958.
18 Y. W. Chen-Yang, Y. T. Chen, H. C. Chen, W. T. Lin and C. H. Tsai, *Polymer*, 2009, **50**, 2856.
19 J. Evans, C. A. Vincent and P. G. Bruce, *Polymer*, 1987, **28**, 2324.
20 H.-M. Kao, T.-T. Hung and G. T. K. Fey, *Macromolecules*, 2007, **40**, 8673.
21 H. M. Kao, S. W. Chao and P. C. Chang, *Macromolecules*, 2006, **39**, 1029.
22 M. M. Coleman, K. H. Lee, D. J. Skrovanek and P. C. Painter, *Macromolecules*, 1986, **19**, 2149.
23 X. H. Flora, M. Ulaganathan, R. S. Babu and S. Rajendran, *Ionics*, 2012, **18**, 731.
24 Y. W. Chen-Yang, H. C. Chen, F. J. Lin and C. C. Chen, *Solid State Ionics*, 2002, **150**, 327.
25 H. W. Chen and F. C. Chang, *J. Polym. Sci., Part B: Polym. Phys.*, 2001, **39**, 2407.
26 N. Sonobe, T. Kyotani and A. Tomia, *Carbon*, 1988, **26**, 573.
27 P. Patnaik, *Dean's Analytical Chemistry Handbook*, McGraw-Hill, New York, 2nd edn, 2004, p. 7.1.

28 D. L. Pavia, G. M. Lampman and G. S. Kriz, *Introduction to spectroscopy*, Harcourt College Publication, USA, 2001, p. 15.
29 J. Eschmann, J. Strasser, M. Xu, Y. Okamoto, E. Eyring and S. Petrucci, *J. Phys. Chem.*, 1990, **94**, 3908.
30 N. K. Karan, D. K. Pradhan, R. Thomas, B. Natesan and R. S. Katiyar, *Solid State Ionics*, 2008, **179**, 689.
31 C.-W. Kuo, C.-W. Huang, B.-K. Chen, W.-B. Li, P.-R. Chen, T.-H. Ho, C.-G. Tseng and T.-Y. Wu, *Int. J. Electrochem. Sci.*, 2013, **8**, 3834.
32 D. Turnbull and M. H. Cohen, *J. Chem. Phys.*, 1961, **34**, 120.
33 D. Turnbull and M. H. Cohen, *J. Chem. Phys.*, 1970, **52**, 3038.
34 D. Saikia, Y.-C. Pan and H.-M. Kao, *Membranes*, 2012, **2**, 253.
35 G. Jiang, S. Maeda, Y. Saito, S. Tanase and T. Sakai, *J. Electrochem. Soc.*, 2005, **152**, A767.
36 S.-K. Kim, D.-G. Kim, A. Lee, H.-S. Sohn, J. J. Wie, N. A. Nguyen, M. E. Mackay and J.-C. Lee, *Macromolecules*, 2012, **45**, 9347.
37 C. W. Nan and D. M. Smith, *Mater. Sci. Eng., B*, 1991, **10**, 99.
38 J. Maier, *Prog. Solid State Chem.*, 1995, **23**, 171.
39 D. Fauteux, *Solid State Ionics*, 1985, **17**, 133.
40 S. Morzilli, F. Bonino and B. Scrosati, *Electrochim. Acta*, 1987, **32**, 961.
41 Y.-H. Liang, C.-C. Wang and C.-Y. Chen, *J. Power Sources*, 2008, **176**, 340.
42 M. Kumar and S. S. Sekhon, *Ionics*, 2002, **8**, 223.
43 R. Kumar, B. Singh and S. S. Sekhon, *J. Mater. Sci.*, 2005, **40**, 1273.
44 M. Ue, *J. Electrochem. Soc.*, 1994, **141**, 3336.
45 S. H. Chung, K. R. Jeffrey and J. R. Stevens, *J. Chem. Phys.*, 1991, **94**, 1803.
46 N. C. Mello, T. J. Bonagamba, H. Panepucci, K. Dahmouche, P. Judeinstein and M. A. Aegerter, *Macromolecules*, 2000, **33**, 1280.
47 A. C. Bloise, J. P. Donoso, C. J. Magon, A. V. Rosario and E. C. Pereira, *Electrochim. Acta*, 2003, **48**, 2239.
48 M. Kunze, Y. Karatas, H.-D. Wiemhöfer, H. Eckert and M. Schönhoff, *Phys. Chem. Chem. Phys.*, 2010, **12**, 6844.